



**Department of Transport and Regional Services
Australian Transport Safety Bureau**

Development and Testing of Production Prototypes of a Protective Headband for Car Occupants

Giulio Ponte, Robert Anderson, Jack McLean and Luke Streeter
Road Accident Research Unit
University of Adelaide

Robert Tiller and Steve Hill
Tiller and Tiller

**AUSTRALIAN TRANSPORT SAFETY BUREAU
DOCUMENT RETRIEVAL INFORMATION**

Report No.	Date	Pages	ISBN	ISSN
CR 210	June 2002	26	0 642 25598 9	1445-4467

Title and Subtitle

Development and Testing of Production Prototypes of a Protective Headband for Car Occupants

Authors

Ponte G, Anderson RWG, McLean AJ, Streeter L, Tiller R and Hill S

Performing Organisations

Road Accident Research Unit
University of Adelaide
SOUTH AUSTRALIA 5005

Tiller and Tiller
Suite 2, Level 2
661 Darling Street
ROZELLE NSW 2039

Sponsored by / Available from

Australian Transport Safety Bureau
PO Box 967
CIVIC SQUARE ACT 2608

Project Officer: John Goldsworthy

Abstract

This report details the results of tests made on a headband designed to protect car occupants in a crash. The tests were performed in a manner such that the headband's effectiveness could be compared with the requirements of the United States Federal Motor Vehicle Safety Standard 201. That standard requires a certain level of head protection for the occupants of the vehicle from the upper interior of the car. The standard stipulates that a free motion headform be fired against the interior components of the car at a speed of up to 24 km/h. The requirement is that a modified value of the Head Injury Criterion, HIC(d), be less than 1000. In these tests a free motion headform was launched at a beam that simulated a structure of a car's interior. The stiffness of the beam was varied, and the headform was fired, first, without any protection, and second, with prototype headbands made of either 70 g/l EPP or 50 g/l EPP. By comparing the impacts in these configurations we found that the headband absorbed significant amounts of energy, reduced peak loads and kept the impact within acceptably safe limits as measured by the Head Injury Criterion. This study showed that the headband similar to that tested would offer significant head protection in frontal impacts. This could offer safety advantages to occupants of older vehicles who otherwise would not benefit from recent advances in occupant protection and also to occupants of more recent vehicles who might be seeking supplementary safety devices.

Keywords

HEAD PROTECTION, HELMET, CAR OCCUPANTS, IMPACT PROTECTION, ENERGY ABSORPTION

NOTES:

- (1) This report is disseminated in the interests of information exchange.
 - (2) The views expressed are those of the author(s) and do not necessarily represent those of the Commonwealth.
-

Reproduction of this page is authorised

Executive summary

This publication is the third in a series of reports for the ATSB in which we have detailed the development of a protective headband for car occupants. In CR193, we documented the results of tests made to determine the energy absorbing characteristics of several candidate materials. CR205 reported further investigations of possible production grade materials and discussed aspects of the design that would determine the general form of the headband in a consumer version of the product.

This report details the results of tests made on the headband, which may be compared with the requirements of the United States Federal Motor Vehicle Safety Standard 201. That standard requires a certain level of head protection for the occupants of the vehicle from the upper interior of the car. The standard stipulates that a free motion headform be launched against the interior components of the car at a speed of up to 24 km/h. The requirement in these tests is that a modified value of the Head Injury Criterion, HIC(d), be less than 1000. The nature of the test required by FMVSS 201 provides a method by which the effectiveness of the headband may be assessed.

In this study, prototype headbands were fabricated according to a design developed in CR205. The energy absorbing element was machined from a solid block of expanded polypropylene and sandwiched between a styrene outer shell and a cloth liner. These prototypes were designed to be dimensionally and materially similar to a future consumer version of the product (should such a version arise).

The aim of the testing was to choose structures that would behave similarly to structures found in the interior of a car. The test structure was designed so that the impact stiffness could be varied. The structure was such that a straightforward execution of the test procedure (without the headband) produced HIC(d) results that ranged from a pass (717), to a moderate fail (1623). The tests were then repeated with a headband attached to the headform so that a comparison of impacts with and without the headband could be made.

Two grades of EPP were evaluated in this study; a 50 g/l density foam and a 70 g/l density foam. The tests showed that headbands manufactured from either grade of EPP provided substantial protection with the most severe impact producing a HIC(d) value of 601 (compared to 1623 for the bare headform in the same test). Further analysis of the dynamic crush characteristics of the headband showed that the 70 g/l EPP was a more efficient energy absorber than the lower density material. This was also reflected in lower HIC(d) values in tests that used the 70 g/l foam. The headband provided protection by limiting peak loads and absorbing significant amounts of energy.

In frontal impacts, the headband would provide significant head protection for car occupants. This would be particularly beneficial for the occupants of older vehicles. Parts of Australia have a median vehicle age around 10 years. That implies that, on current trends, it will take 10 years before a new vehicle safety feature, introduced today, will be present in half the car fleet in this country. The headband may provide the drivers of older cars some of the benefits of new safety features immediately. We expect that there would also be benefits for the occupants of newer cars, as the headband would provide protection from striking objects that are not protected by padding or airbags.

Table of contents

Executive summary	iii
Table of contents	iv
1. Introduction	1
1.1. Aims	1
2. Prototype design and production	2
3. Test methods	3
1.2. Headband attachment	5
1.3. Test measurements	6
1.3.1. Head velocity	6
1.3.2. Head acceleration	6
1.3.3. Dynamic crush	7
1.3.4. High speed video	7
1.4. Test matrix	7
4. Results	9
1.5. Head Injury Criterion	9
1.6. Headform acceleration	9
1.6.1. Force - deflection measurements	13
1.6.2. Comparison of high speed video with force-deflection measurements	15
5. Discussion and conclusions	17
6. References	18
Appendix: High-speed video and force-deflection curves for each headband test	

1 Introduction

McLean et al (1997) proposed a protective headband for car occupants in a report to the Federal Office of Road Safety (CR160). The report investigated the benefits of interior padding designed to prevent head injuries to car occupants. The report was prompted by the National Highway Traffic Safety Administration's proposed changes to the US Federal Motor Vehicle Safety Standard (FMVSS) 201 to include a minimum level of head protection in impacts with the upper interior of the passenger compartment. The amendment required all new cars to have a specified level of head impact protection by the year 2002. This is being implemented largely through the use of interior padding. The report estimated that head protection similar to a pedal cycle helmet would be more effective than vehicle padding for reducing head injuries in the event of a crash. It was proposed that a headband constructed of energy absorbing material covering the forehead and sides of the head would also provide a significant amount of head protection (though only providing half the protection of a bicycle helmet). The headband that was proposed would also be less cumbersome for car occupants than a pedal cycle helmet and would benefit the occupants of vehicles that had no additional interior occupant protection.

Anderson et al. (2000) detailed the results of testing of numerous materials that could be considered in the construction of a protective headband. The report concluded that an energy absorbing headband could provide significant benefits by reducing head injuries to car occupants involved in a collision. In a subsequent study, Anderson et al. (2001) detailed the results of further tests on alternative energy absorbing materials. A design development process guided the selection of materials for testing, and the design process was also documented in the report. The report made a recommendation to do further evaluations of expanded polypropylene (EPP) as it displayed desirable energy absorbing characteristics and durability.

This report evaluates the performance of a production prototype of a headband constructed using EPP. The report details the construction of the prototype and the testing thereof. The report goes on to discuss the results of the testing and makes recommendations for the direction of continued development.

1.1 AIMS

The aims of the study were to:

- Produce a functional prototype of a protective headband for car occupants using materials selected on the basis of Anderson et al. (2001),
- Examine the effectiveness of the headband using a standard test procedure, and
- Report and discuss the results obtained from the tests and make necessary recommendations for continued development.

2 Prototype design and production

Anderson et al. (2001) recommended further evaluation of expanded polypropylene (EPP) for use in the headband as it exhibited desirable energy absorbing characteristics and durability. Eight prototype headbands were fabricated using EPP as the energy absorbing element, four using EPP with a density of 70 g/l and four using EPP with a density 50 g/l. The prototypes consisted of the energy-absorbing EPP foam, lined with a cloth fabric on the interior surface, and a vacuum formed styrene shell on the forward exterior surface (see Figure 2.1). The design included an adjustable elastic strap for securing the headband to the head.

The EPP component of the headband was fabricated using a computer numerical control (CNC) machining process, in which pre-cast foam blocks of the correct density were cut to shape.



Figure 2-1 The headband is constructed from a layer of energy absorbing expanded polypropylene and a vacuum formed styrene shell

3 Test methods

Vehicles sold in the United States will, from 2002, be required to comply with those parts of FMVSS 201 requiring a minimum level of head impact protection. It is expected that car manufacturers will meet the standard by padding the upper interior of the car. The intention of the headband is to provide a level of head protection for occupants that is independent of that provided by car manufacturers (McLean et al., 1997). However, FMVSS 201 provides a method to evaluate the level of protection provided by the headband to an occupant in the event of an impact with interior components of a vehicle during a crash. The use of the procedures in FMVSS 201 also allows the headband to be evaluated alongside other measures designed for occupant head protection.

FMVSS 201 stipulates the use of a free motion headform (Part 572 Subpart L) launched at a speed of 19km/h or 24km/h, depending on the structure being tested. The performance criterion of FMVSS 201 is that a modified form of the Head Injury Criterion, HIC(d), should be less than 1000. The HIC(d) calculation takes into account the fact that the free motion headform is not attached to a dummy. The modification of the HIC is an attempt to give an equivalent dummy HIC without the need for a full crash test and a complete crash test dummy.

The HIC(d) modification is given as:

$$\text{HIC(d)} = 0.75446(\text{HIC}) + 166.4 \quad (\text{Equation 1})$$

where

$$\text{HIC} = (t_2 - t_1) \frac{\int_{t_1}^{t_2} a dt}{t_2 - t_1}^{-2.5} \quad (\text{Equation 2})$$

Where t_1 and t_2 are chosen to maximize the function.

3.1 IMPACT CONFIGURATION

For this study, a steel beam was used to simulate a component of the interior of a vehicle. The beam was designed so that its stiffness could be varied. The advantage of using this beam was that it could sustain repeated impacts without any local plastic deformation (unlike real interior vehicle components). It was designed to be an effective way of attaining repeatable results from the impact tests.

The steel beam comprised two lengths of mild steel (90° sections) and a sandwiched flat bar of mild steel. The assembly was joined by a series of screws. This structure formed a “T” section beam. The beam was clamped at each end to two short steel box sections. These beam clamps were supported by two longer support rails. This construction allowed the stiffness of the beam to be changed by varying the thickness of the flat bar of mild steel and by adjusting the distance between the two beam clamps. (Figures 3.1 and 3.3)

The Road Accident Research Unit's pedestrian legform launcher was modified to launch the free motion headform (Part 572 Subpart L). The headform was attached to a plate by vacuum pressure and the plate was connected to the carriage system of the launcher. The carriage system is attached to a series of elastic cords which are put into tension as the carriage is drawn back hydraulically. The energy in the elastic cords provides the kinetic energy required to give the impactor the desired impact speed. The speed of the impactor is measured using a dual laser beam system (Section 3.3.1).

The steel beam construction was rigidly fixed at an angle of 20 degrees from the vertical (Figures 3.1 to 3.3). The beam was set at this angle so that during the impact with the steel beam, the normal force provided by the beam passed through the centre of gravity of the headform.



Figure 3-1 A photograph of the launcher and the beam fixed in position.

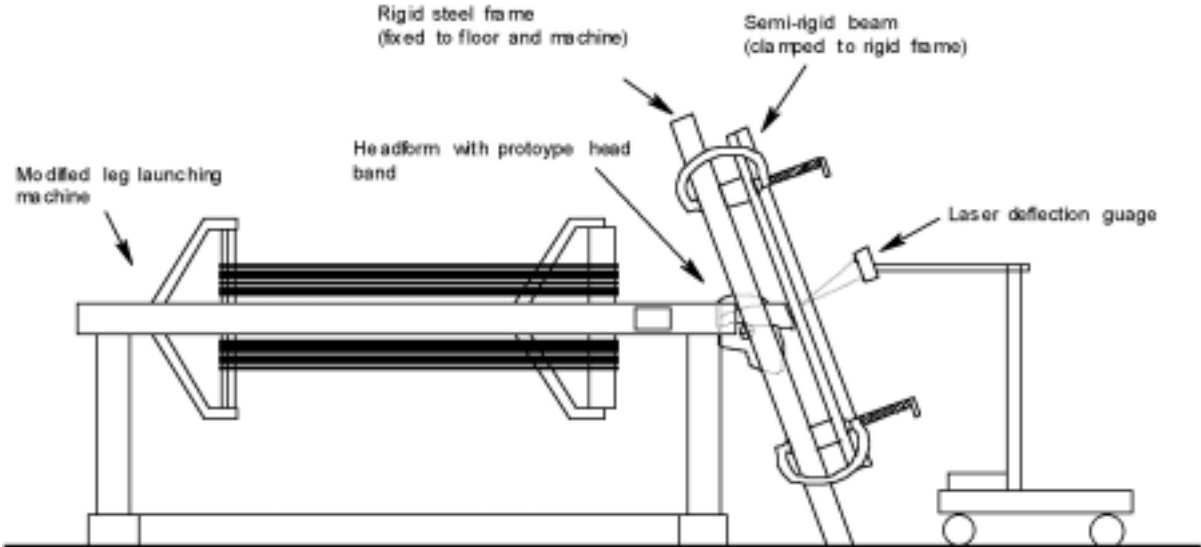


Figure 3-2 Experimental set-up of the launcher with headform and headband shown at the moment of impact.



Figure 3-3 Test set-up with the headform, headband and beam in position prior to a test.

3.2 HEADBAND ATTACHMENT

The prototype headband was designed to fit the head of a 50th percentile male. The free motion headform, although nominally that of a 50th percentile male, did not provide a close mating fit with the headband. Consequently when the headband was attached to the headform there were significant gaps between the headband and the headform (see Figure 3.4). These gaps around the headform would have influenced the dynamic behaviour of the headband, subjecting the headband to three-point bending during impact. The effect of this loading would have been to cause the headband to fail in bending, rather than by crushing (the intended mode of energy absorption).

Bending failure was avoided by the fabrication of a stiff insert of a glass bead filled epoxy resin. The insert provided a mating fit between the headform and the headband, and a uniformly distributed load path. This ensured that the load was distributed across the front of the headform during the impact and that only the thickness and the properties of the EPP were involved in determining the impact behaviour of the headband.



Figure 3-4 The headband attached to the headform. The last image shows the gaps between the headband and the headform that were filled with the insert.

3.3 TEST MEASUREMENTS

The tests were designed to determine the benefit of the headband by comparing the results of impact tests between the free motion headform and the beam, made with and without the headband. The benefit can be summarised by comparing the HIC(d) values in each test. Further, a study of the force-deflection behaviour of the headband was made to explain the mechanism of protection and to identify the better performing material.

3.3.1 Head velocity

The velocity of the headform was measured in every test using a dual-beam laser measurement system. The system consists of two laser diodes separated by a known distance, set parallel to one another and in line with two receivers. The laser receivers are connected to a counter-timer. The lasers and receivers were set so that the headform would break each of the laser beams in succession just before impact. The counter-timer recorded the interval between these events. The impact velocity was calculated by dividing the distance between the lasers by the time elapsed between the two laser signals.

3.3.2 Head acceleration

The Part 572 Subpart L free motion headform was instrumented with a critically damped Entran triaxial accelerometer (see Figure 3.5). The impact acceleration was recorded using a high-speed data acquisition system sampling at 50 kilosamples per second after being filtered with a 10 kHz anti-aliasing filter. The acceleration signals were then conditioned to CFC 1000 (SAE J211 MAR95 - Instrumentation for Impact Test - Part 1 - Electronic Instrumentation).

The resultant acceleration was subsequently used to calculate HIC (Equation 2) and HIC(d) (Equation 1).

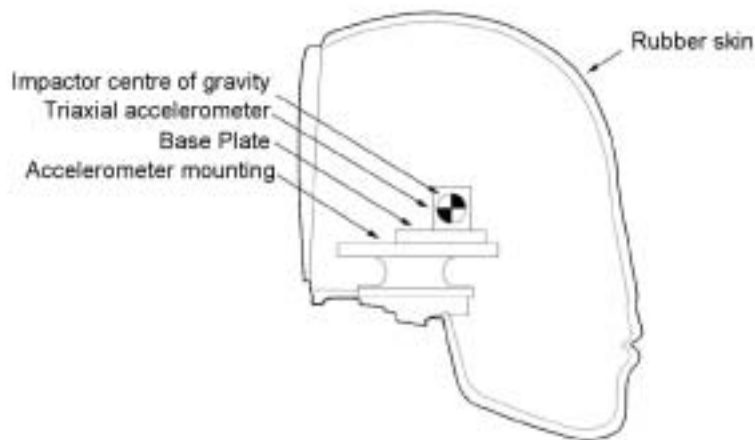


Figure 3-5 A schematic view of the free motion headform.

3.3.3 Dynamic crush

The dynamic crush of the headband was measured to construct a force-deflection curve from each test. The crush in the headband was approximated by determining the difference between the displacement of the headform (assuming no significant skin displacement or headform deformation) and the displacement of the beam. The displacement of the beam was measured in each impact test by a laser deflection gauge (see Figure 3-2). The displacement of the headform during the impact was calculated by the double integration of the acceleration-time history.

3.3.4 High speed video

A high speed digital video camera captured the impact in each test. Impacts were captured at 500 frames per second. These images were used to examine the behaviour of the headband and the rotation of the headform during the test.

3.4 TEST MATRIX

Six EPP prototype headbands were tested. Three headbands were constructed from 70 g/l EPP and three from 50 g/l EPP. Tests were conducted using three variations in the stiffness of the beam such that the unprotected headform, when fired at 24km/h, would give nominal HIC values of 2000 (Beam 1), 1500 (Beam 2) and 800 (Beam 3). Two of these HIC levels fail the requirements of FMVSS 201 and the other passes, giving a range of severities around the pass/fail criterion in the standard.

The lowest HIC level of 800 is similar to a result obtained from a previous test; that was made with a section of B-Pillar from a 1978 Toyota Corolla. Two tests from Anderson et al (2001) were made using an unprotected aluminium headform, striking the B-Pillar at 23.4km/h and 23.3km/h. The HIC values measured in those tests were 822 (Peak Acceleration 225g) and 858 (Peak Acceleration 212g) respectively.

The beam configurations were altered by changing the thickness of the middle steel bar and by varying the support distances. These changes varied the flexural stiffness of the beam. The design and construction of the beam was such that no significant local deformation or significant strain hardening at the impact location occurred. It was assumed that each test on a particular beam was completely independent and unaffected by other tests on the same beam.

4 Results

A summary of the results of the tests is given in Table 4-1.

Table 4-1 Results of the free motion headform impact tests on the different beams

	Test Configuration	Test No.	Peak Acceleration (g)	HIC	HIC(d)	Velocity (km/h)
Beam 1	No Headband	24050202	340	1930	1623	23.2
	Headband (70 g/l)	24050203	110	514	554	23.4
	Headband (50 g/l)	24050204	136	576	601	23.3
Beam 2	No Headband	23050200	286	1437	1251	24.0
	Headband (70 g/l)	23050201	105	497	541	24.0
	Headband (50 g/l)	23050202	128	540	574	24.0
Beam 3	No Headband	23050204	278	730	717	23.6
	Headband (70 g/l)	23050205	73.1	358	436	23.6
	Headband (50 g/l)	23050206	83.7	364	441	23.6

4.1 HEAD INJURY CRITERION

Impacts which generate HIC(d) values in excess of 1000 are considered unacceptably severe and fail according to the performance criterion specified in FMVSS 201. Both densities of the expanded polypropylene prototype headband gave high levels of protection to the free motion headform as measured by HIC(d). The 70 g/l headband performed slightly better than the 50 g/l, but in all cases there was a significant reduction in HIC and HIC(d). For tests made with the beams that generated HIC(d) values in excess of 1000 in the unprotected headform, the headband produced at least a 54 percent reduction in the values of HIC and HIC(d).

A comparison of the results for each beam and each test configuration is made in Figures 4.1 and 4.2. For Beam 1 the HIC reductions were 73 percent and 70 percent for the 70 g/l and the 50 g/l prototypes. The HIC(d) reductions were 66 percent and 63 percent. For Beam 2 the HIC reductions were less marked. The reductions in HIC were 65 percent and 62 percent for the 70 g/l and the 50 g/l prototypes, and the reductions in HIC(d) were 57 percent and 54 percent. The reductions in HIC for Beam 3 were 64 percent for both the 70 g/l and the 50 g/l prototypes, and the reductions in HIC(d) were 39 percent and 38 percent.

4.2 HEADFORM ACCELERATION

Both the 70 g/l and 50 g/l expanded polypropylene prototype headbands significantly reduced peak acceleration in all the headform impacts. The 70 g/l headband reduced the peak acceleration to a greater extent than the 50 g/l headband, although the smallest reduction in peak acceleration by any headband was 55 percent. All other reductions were at least 60 percent, with a maximum reduction of 74 percent.

Each of the following figures (Figures 4.3 to 4.5) shows the acceleration of the headform over the duration of the impact. The acceleration-time curve illustrates the dynamics of the impact.

In the beginning of each impact the curves have a similar gradient irrespective of the presence or type of headband material. This is likely to be the acceleration produced as the head skin deforms; prior to the crushing phase, the EPP is stiffer than the head skin. Once the head skin is fully deformed, the deformation of the headband foam is the dominant influence on the acceleration of the headform.

The 70 g/l headband is stiffer than the 50 g/l headband. As a result of this characteristic, the 70 g/l headband produces a higher acceleration than the 50 g/l headband in the initial stages of the impact. However, the 70 g/l headband allows the acceleration of the headform to peak at lower levels because it absorbs the energy of the impact more efficiently than the 50 g/l material. It is also able to absorb more energy before “bottoming out.”

Because the 50 g/l EPP is a lower density material, it absorbs less impact energy. Once it bottoms out, the headband can no longer absorb much energy. After this time the peak acceleration is influenced primarily by the interaction between the headform and the beam and the remaining energy of the headform. As a result the acceleration peaks higher than the 70 g/l tests.

The effect of the deformation characteristics of the material is discussed further in Section 4.3.

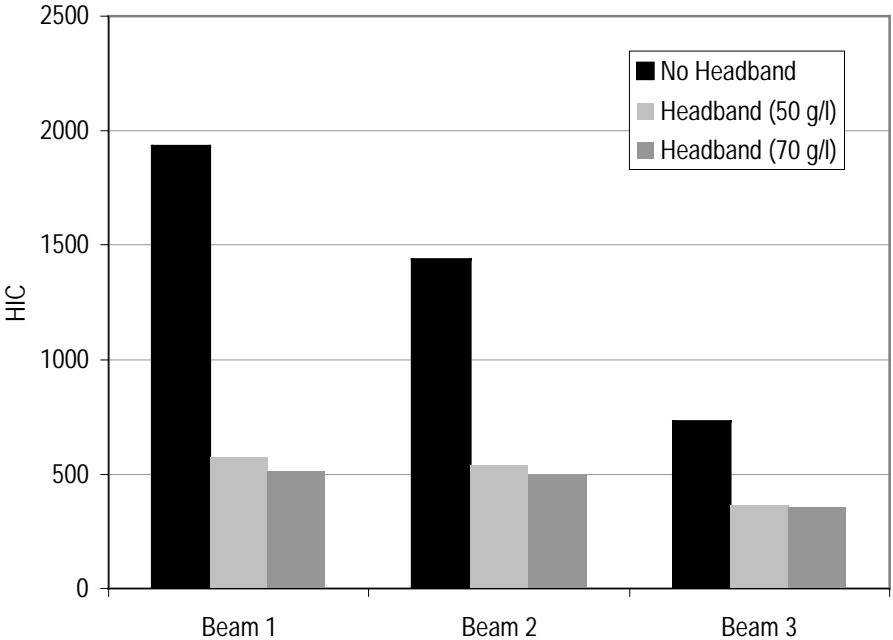


Figure 4-1 Chart showing the Head Injury Criterion results of the tests. The headband significantly reduced the severity of the impact between the headform and the beam.

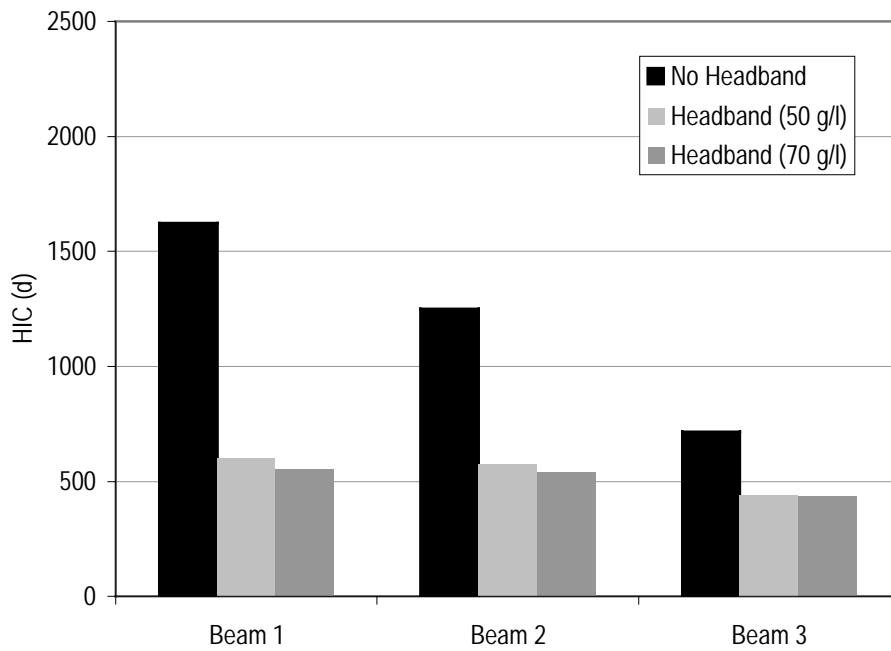


Figure 4-2 Chart showing the Head Injury Criterion (d) results of the tests. HIC(d) is a modified form of HIC to compensate for the free motion of the headform. The headband significantly reduced the severity of the impact as measured by HIC(d).

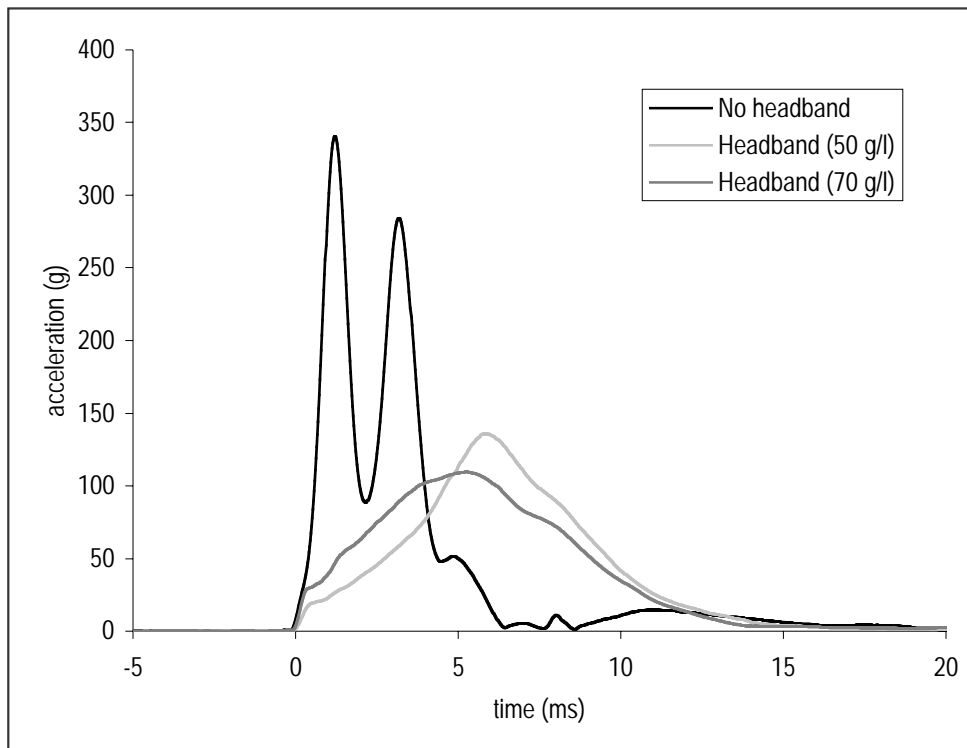


Figure 4-3 Headform acceleration measured in tests against Beam 1.

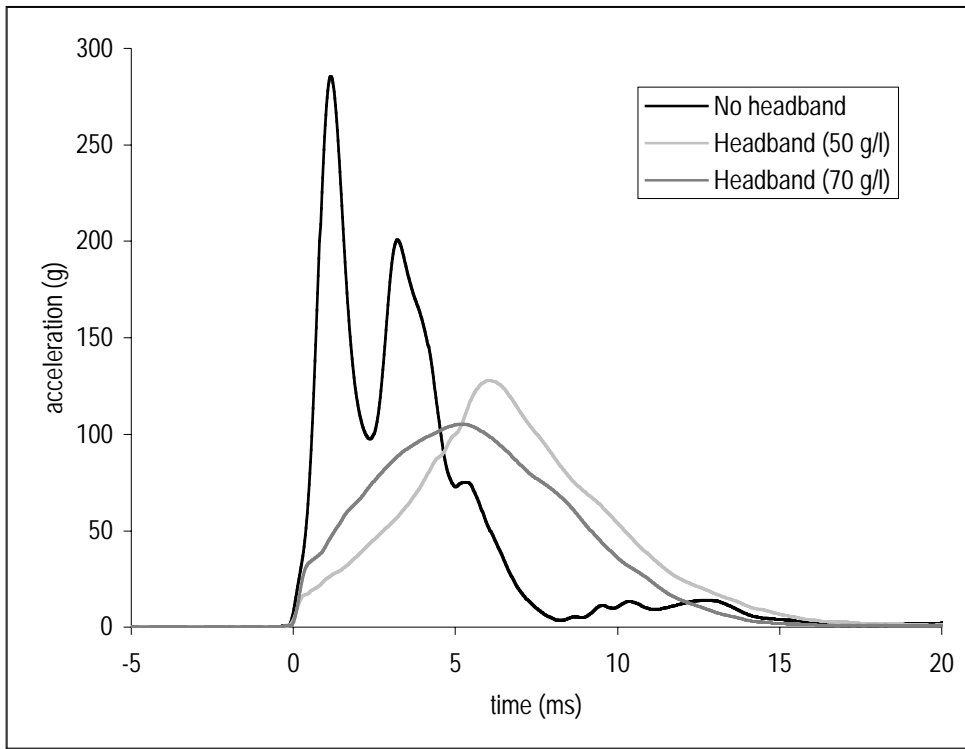


Figure 4-4 Headform acceleration measured in tests against Beam 2.

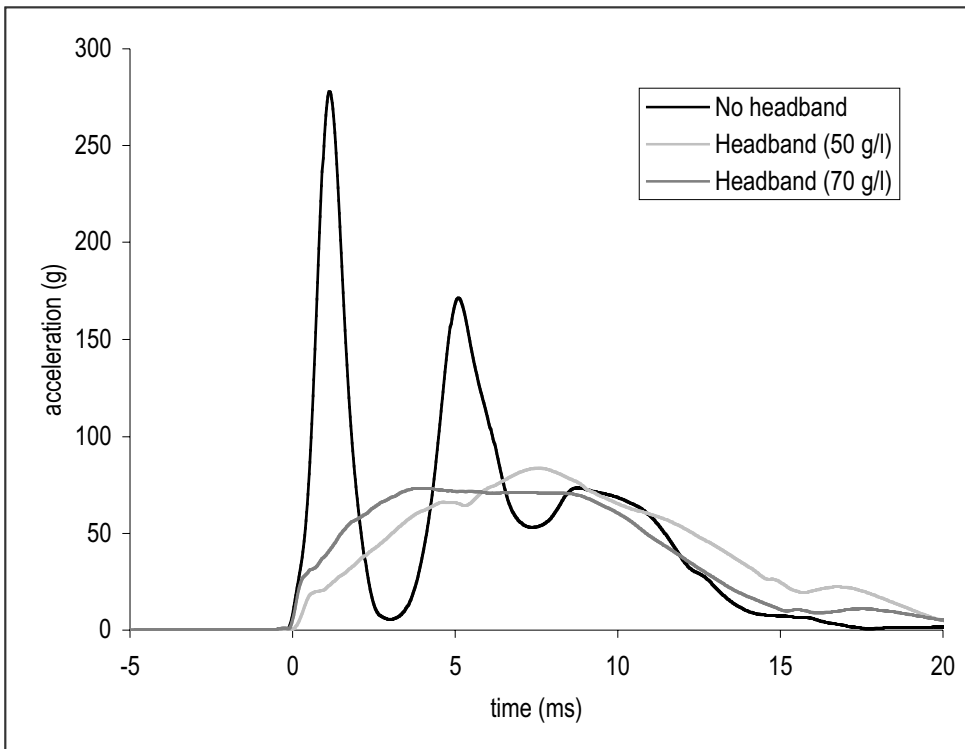


Figure 4-5 Headform acceleration measured in tests against Beam 3.

4.3 FORCE - DEFLECTION MEASUREMENTS

As discussed in Section 3.3, the amount of crush in the headband was approximated by the difference between the displacement of the headform and the displacement of the beam. The displacement of the headform was calculated by the double integration of the acceleration-time history. The beam deflection was measured using a laser deflection gauge. The force history for each impact was calculated by taking the product of the mass and the acceleration of the headform. Each of the following figures (Figures 4.6 to 4.8) shows the resulting force-displacement curves for each headband impact, with the curve for the unprotected headform, calculated in the same manner, included for reference.

In the beginning of each impact, the curves for the unprotected headform and each of the headbands have almost the same gradient. As discussed previously, this part of the curve shows the stiffness of the headskin deformation, which deforms at lower levels of force than required to crush the EPP in the headband.

The peak force for each curve should correspond to the maximum deformation of the headband. It may be observed that the displacement continues to increase beyond the measurement of the peak load. This increase is not related to the crush of the headband, but to the rotation of the headform. Inspection of the high-speed video reveals that the rotation of the headform becomes significant at some point beyond the peak force (Section 4.4). On this basis, these curves should be considered valid only in the loading part of the curve.

The 70 g/l headband caused higher initial forces than the 50 g/l headband. Ultimately, however, it compressed less and the forces peaked at a lower level than the 50 g/l headband. The 50 g/l headband appeared to bottom out before maximum loading in tests with Beam 1 and Beam 2. At this point the headband could not significantly absorb any more energy. As a consequence the headform protected by the 50 g/l headband sustained higher loads than when protected by the 70 g/l headband.

The force-displacement curves also indicate the amount of work done (or energy absorbed) by the headband in each test. The work done is the area under the force-displacement curve. On inspection, it is also clear that the 70 g/l EPP headband is a more efficient energy absorber than the 50 g/l EPP headband, absorbing more energy throughout the crushing phase of the impact.

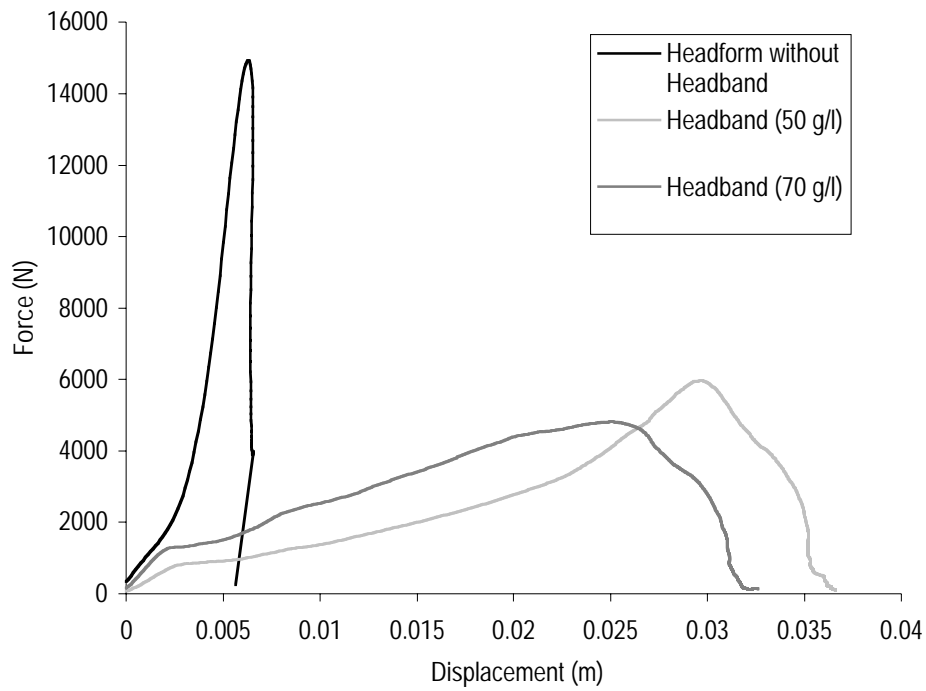


Figure 4-6 The force - displacement curves for the headband in the impacts with Beam 1. The deflection in the unprotected headform is included for reference.

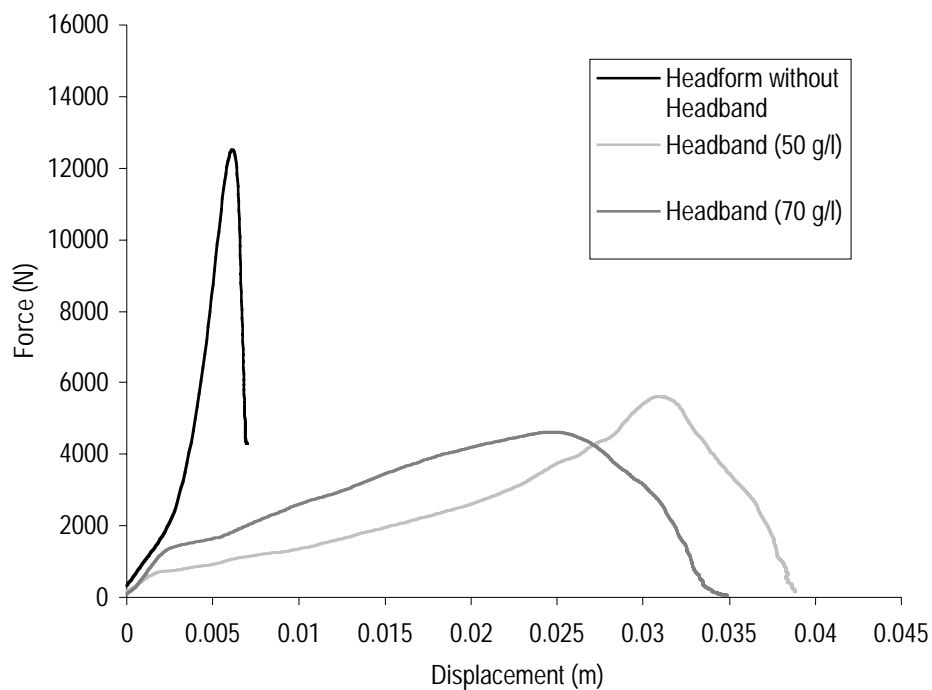


Figure 4-7 The force - displacement curves for the impacts with Beam 2. The deflection in the unprotected headform is included for reference.

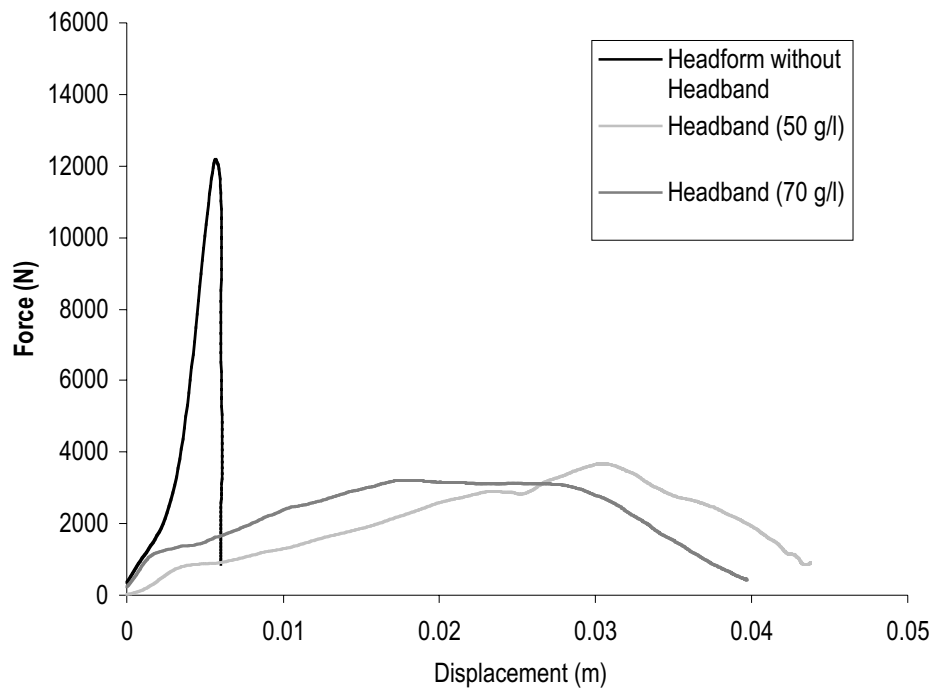


Figure 4-8 The force - displacement curves for the impacts with Beam 3. The deflection in the unprotected headform is included for reference.

4.4 COMPARISON OF HIGH SPEED VIDEO WITH FORCE-DEFLECTION MEASUREMENTS

A high speed digital video camera was used to capture images of each test. Video was captured at 500 frames per second. The video provides a direct comparison between the kinematics of the headform and the force-deflection curves. Figure 4.9 shows the high speed film images for test 23050201, in which the 70 g/l headband was attached to the headform and fired at Beam 2. Figure 4.10 shows the force-deflection curve for the same test, with the curve labeled with the time that had elapsed from the beginning of the impact.

The high speed film image at 0 ms is the first point of contact between the headband and the beam as recorded on the video. With reference to Figure 10, the impact load peaks just before the 6 ms mark. The peak load corresponds to approximately 25 mm of compression. With reference to Figure 9, the headband appears to be exhibiting maximum deformation at around 6 ms, corresponding with the time of the peak force.

After 6 ms the headform rotation becomes visible in the video image, and the extent of the rotation can be observed in each of the frames following this time. The force-deflection curve beyond 6 ms is therefore likely to be inaccurate, as the headform rotation causes the displacement measurement to become indeterminate.

The high speed film images and corresponding force-deflection curves for the other headband tests are presented in an Appendix to this report.

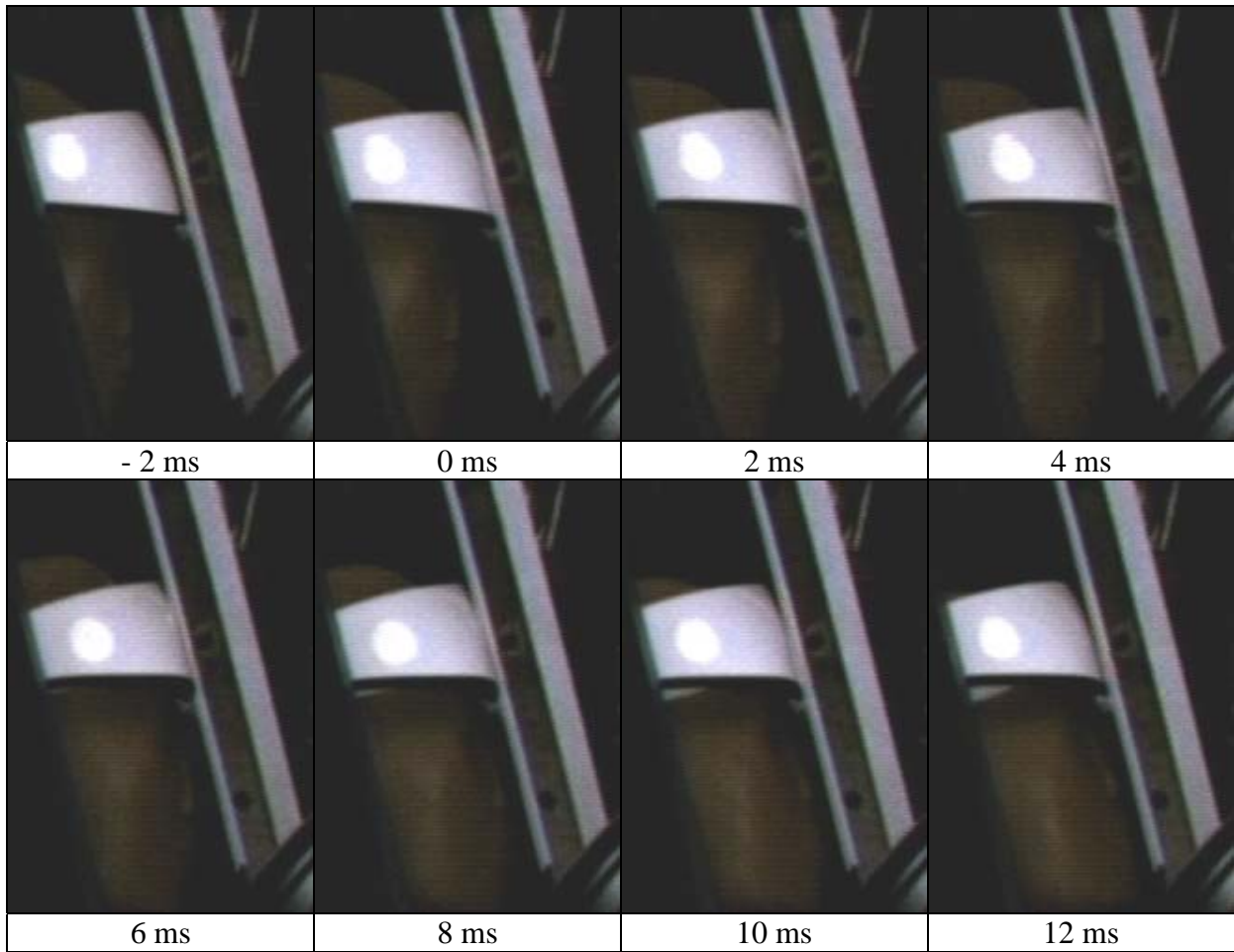


Figure 4-9 High speed film images for test 23050201.

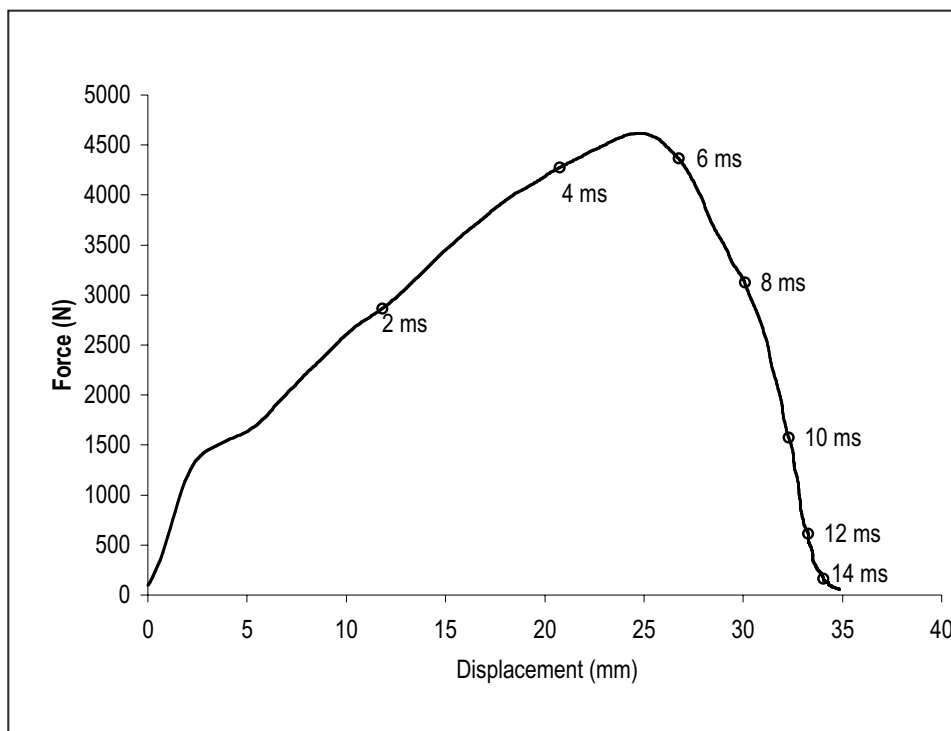


Figure 4-10 The force - displacement curve of the headband calculated from the results of test 23050201.

5 Discussion and conclusions

The headband prototypes provided protection to the free motion headform in all the tests conducted, to the extent that the criterion for acceptance under FMVSS 201 was satisfied. Three different levels of stiffness were tested. Two of the beam stiffnesses were such that they failed the minimum performance criteria of the FMVSS 201 (i.e. that $HIC(d) < 1000$) when tested with the unprotected headform. When either of the headbands were attached to the free motion headform, the $HIC(d)$ was reduced to acceptable levels. The headbands also reduced the peak acceleration of free motion headform considerably.

Although both the 70 g/l and 50 g/l prototype headbands surpassed the requirements of FMVSS 201, the 70 g/l prototype headband performed better than the 50 g/l in all tests. The 70 g/l prototype absorbed more energy and absorbed it more efficiently than the 50 g/l prototype.

It should be noted that the performance of the headband has only been assessed in this report for frontal impacts through the centre of the headband. In this part of the headband the material thickness is at a maximum. In the design evaluated here, the material thickness gradually decreases around the headband to a minimum at the sides. Anderson et al. (2001) recommended a minimum material thickness of 25 mm, however the current prototype design incorporates a thickness below this minimum for aesthetic reasons.

Future design evaluation will need to consider material thickness and coverage issues and it would be of benefit to conduct side impact tests to ensure that adequate protection is provided in this impact direction. Future evaluation might also include the use of a crash test dummy in a sled or full-scale crash test. Examining the protective effects in these situations at speeds higher than those examined here would be informative for further evaluation of the headband's protective effect. Other factors that might be considered include fitment of the headband, and the importance of correct attachment of the headband to the head.

McLean et al. (1997) estimated "that it would be more than 15 years from the time that a decision was made to require padding before half of the cars on the road in Australia provided such protection against head injury." With this in mind, it is important to consider more immediate options to protect against possible head injury in vehicle crashes. McLean et al. (1997) estimated that pedal cycle helmets could provide better protection than could be offered by interior padding. In the same study it was also estimated that a headband covering the sides of the head and the forehead, while providing half the benefits of a pedal cycle helmet, would offer more protection than interior padding.

This study documents tests and results that demonstrate the effectiveness of a headband of the sort originally proposed in 1997. The benefits of wearing a headband similar to the one evaluated in this report would be considerable, on the basis of the results of the tests reported herein.

6 References

McLean, A.J., Fildes, B.N., Kloeden, C.N., Digges, K.H., Anderson, R.W.G., Moore, V.M. & Simpson, D.A. (1997). Prevention of Head Injuries to Car Occupants : An investigation of Interior Padding Options. Report No. CR160, Federal Office of Road Safety, Canberra.

Anderson, R.W.G., White, K. & McLean, A.J. (2000). The Development of a Protective Headband for Car Occupants. Report No. CR193, Australian Transport Safety Bureau, Canberra.

Anderson, R.W.G., Ponte, G. & McLean, A.J. (2001). Further Development of a Protective Headband for Car Occupants. Report No. CR205, Australian Transport Safety Bureau, Canberra.

Appendix: High-speed film and force-deflection curves for each headband test

This section presents the high speed video images of each headband test and the associated force-deflection curves.

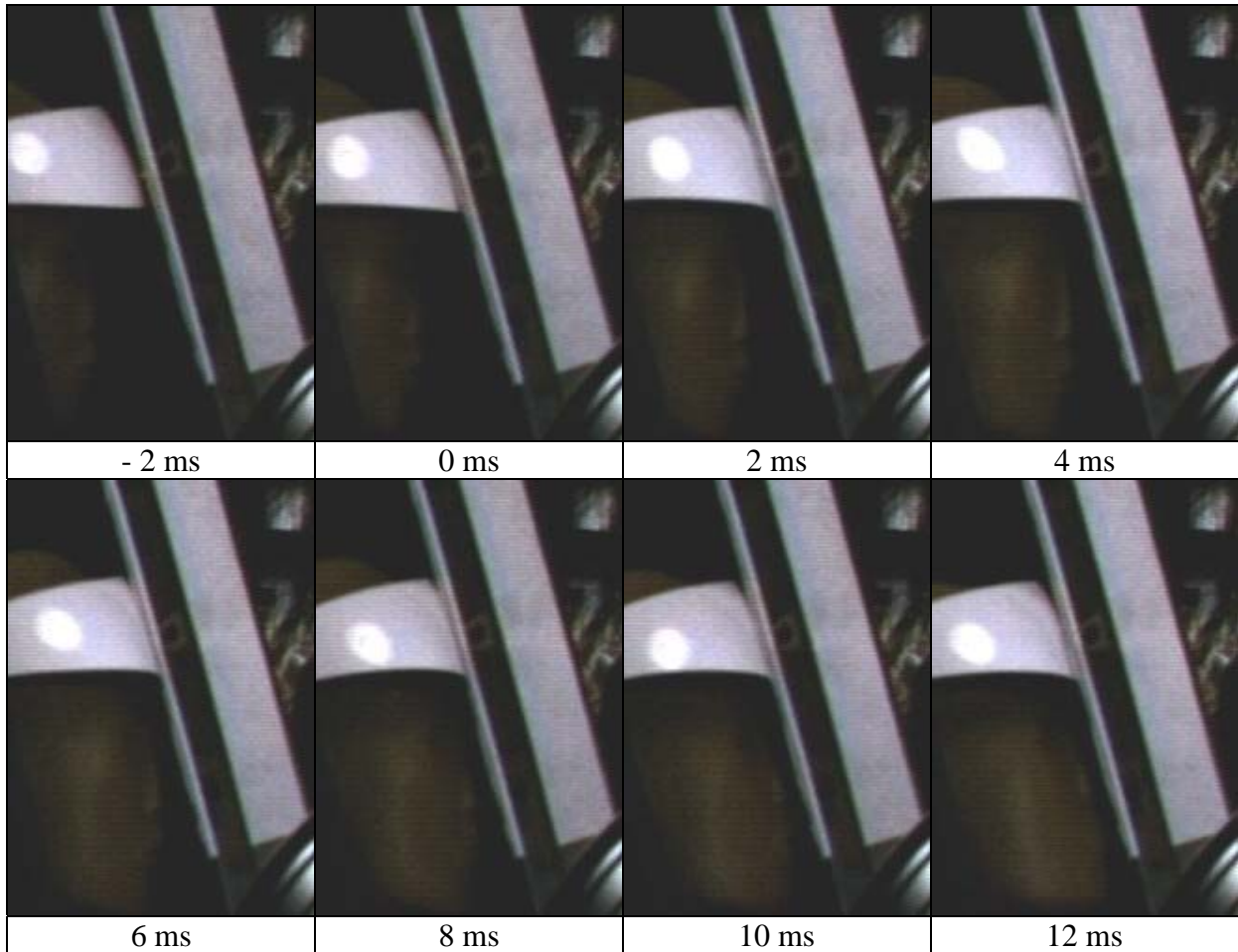


Figure A-1 High speed video images for test 24050203. (70 g/l headband, Beam 1)

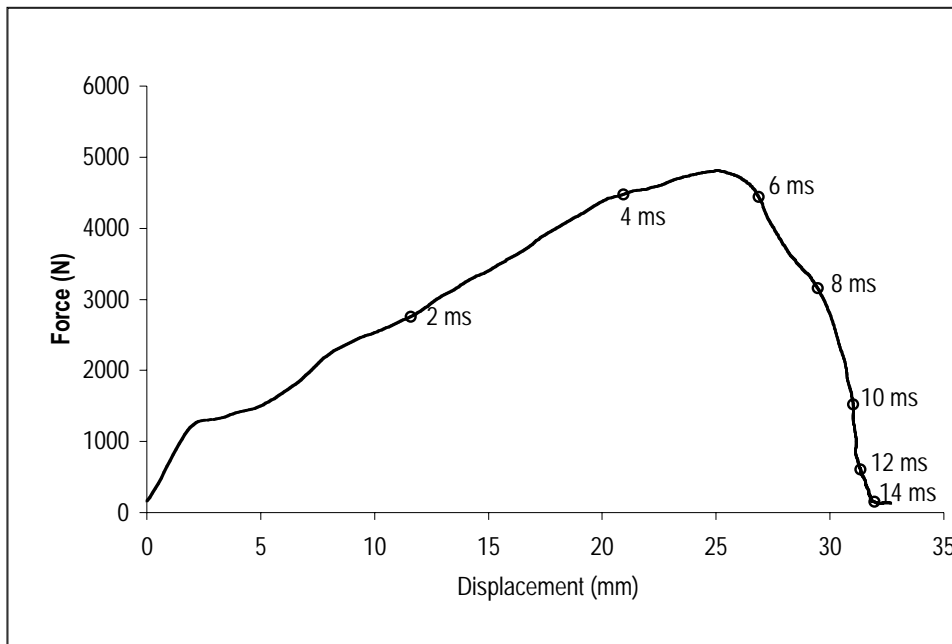


Figure A-2 The force - deflection curve for test 24050203. (70 g/l headband, Beam 1)

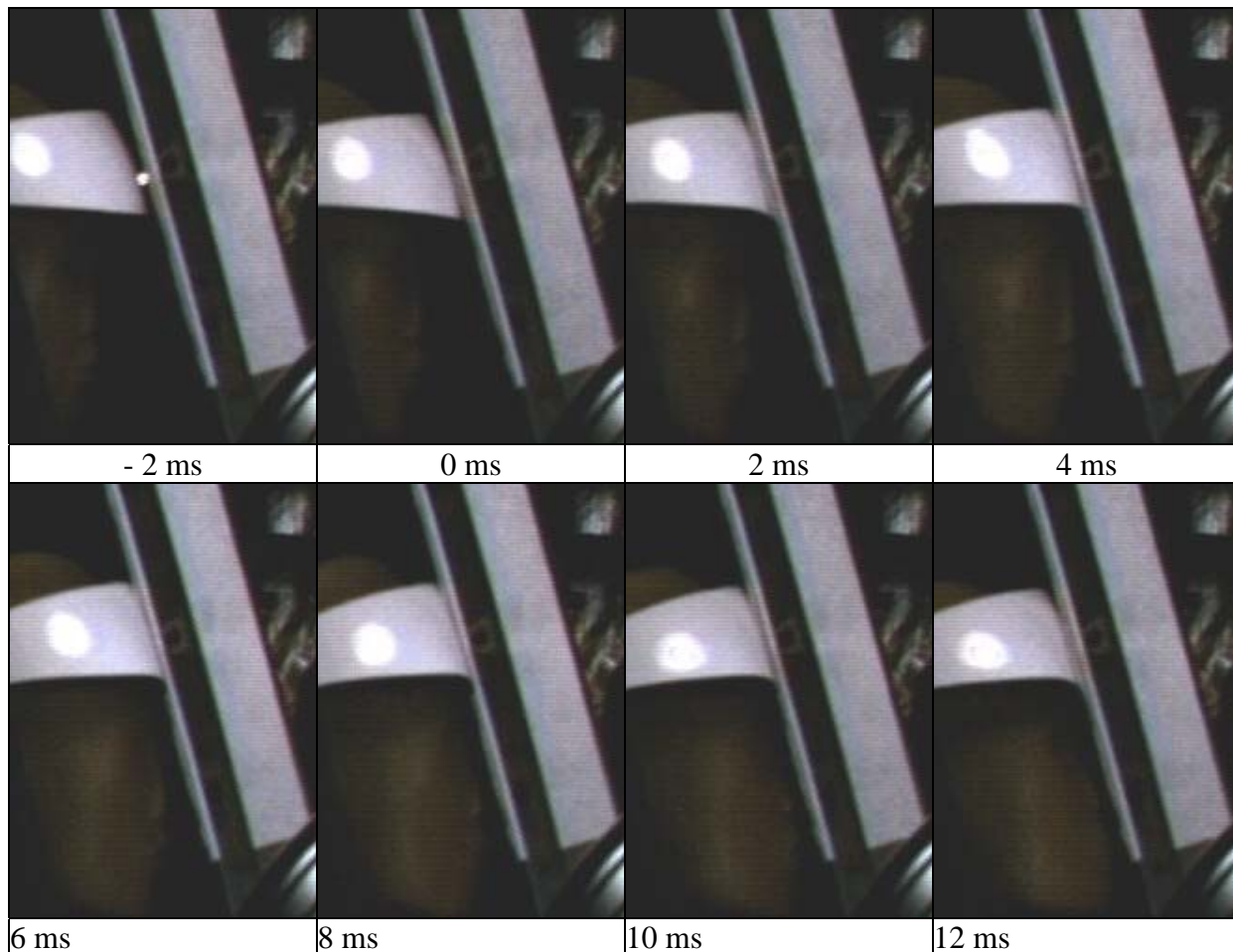


Figure A-3 High speed video images for test 24050204. (50 g/l headband, Beam 1).

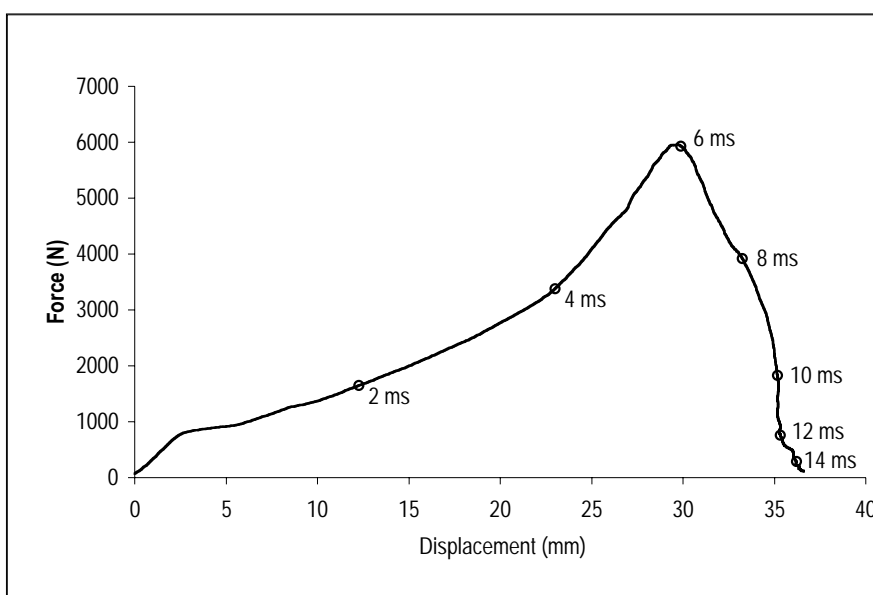


Figure A-4 The force - deflection curve for test 24050204. (50 g/l headband, Beam 1).

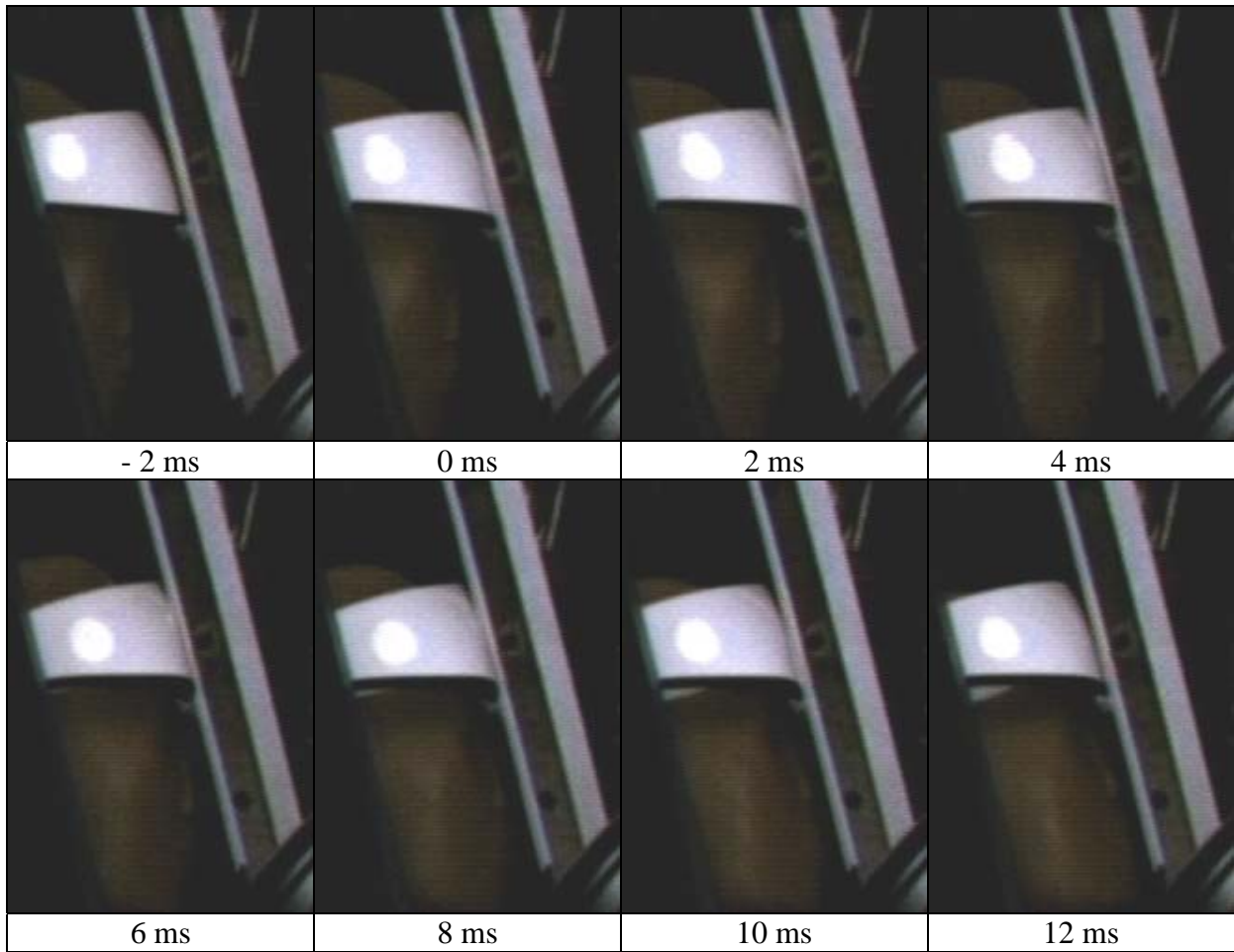


Figure A-5 High speed film images for test 23050201. (70 g/l headband, Beam 2)

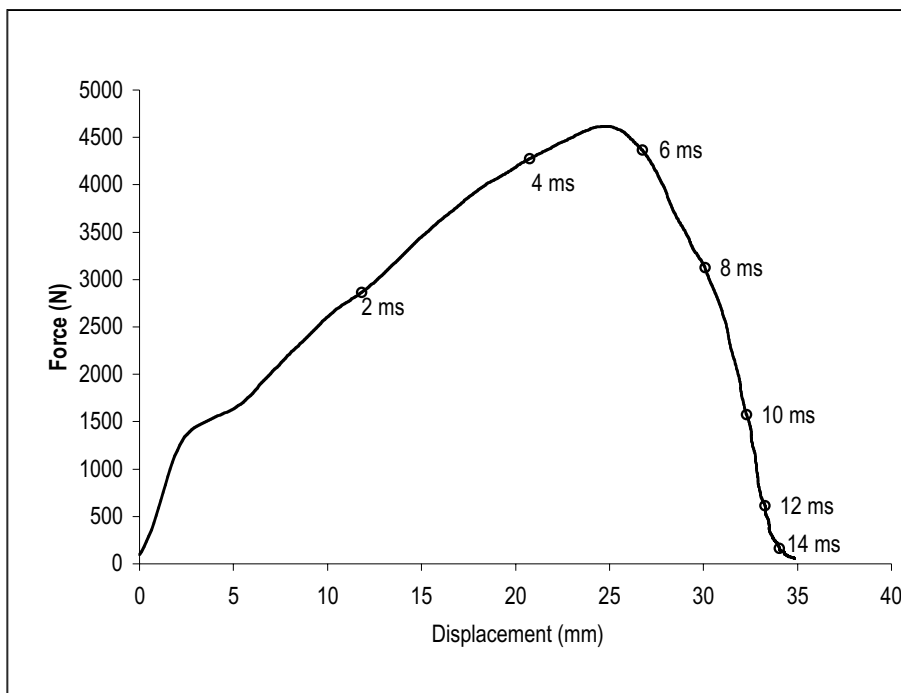


Figure A-6 The force - deflection curve for test 23050201. (70 g/l headband, Beam 2).

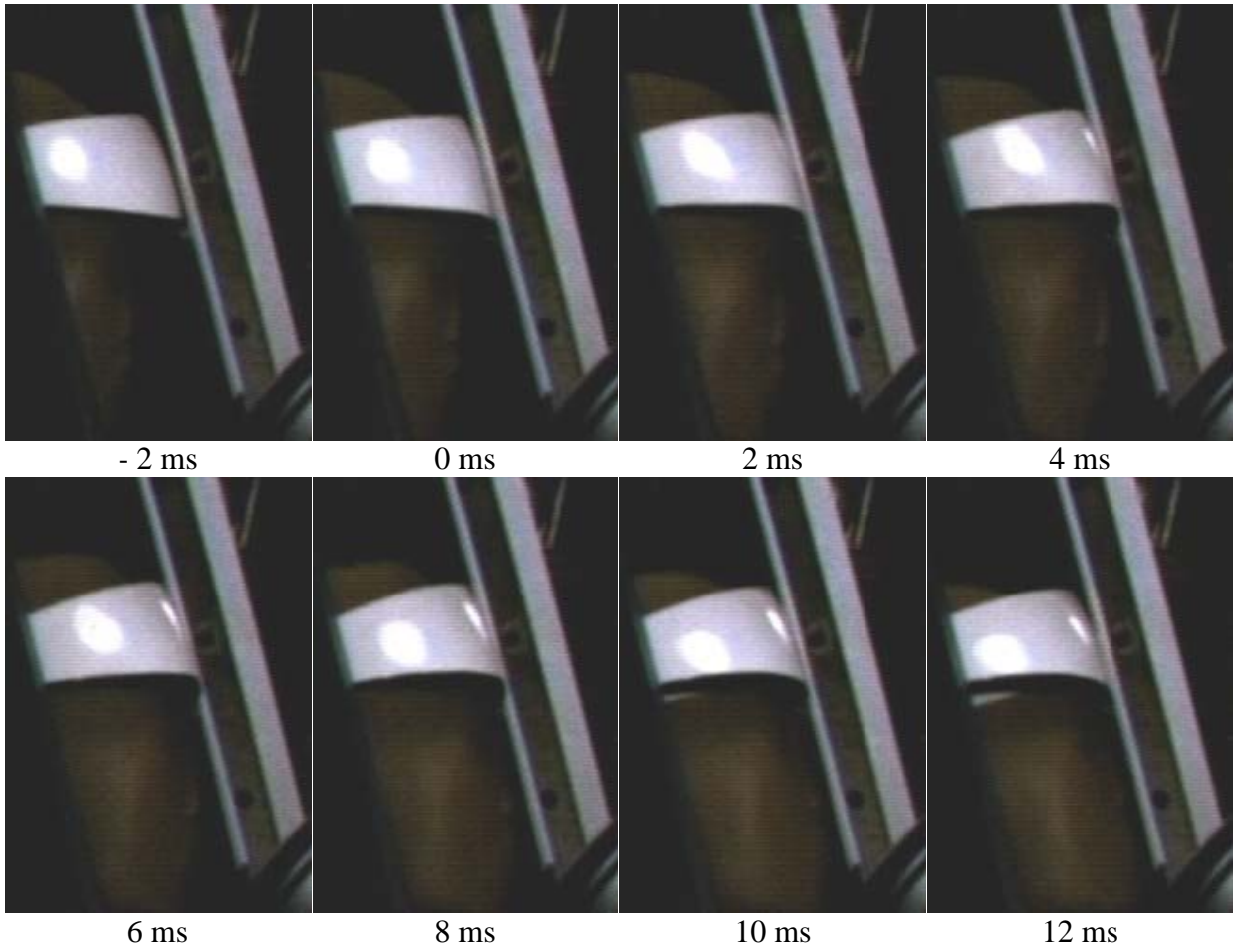


Figure A-7 High speed video images for test 23050202 (50 g/l headband, Beam 2)

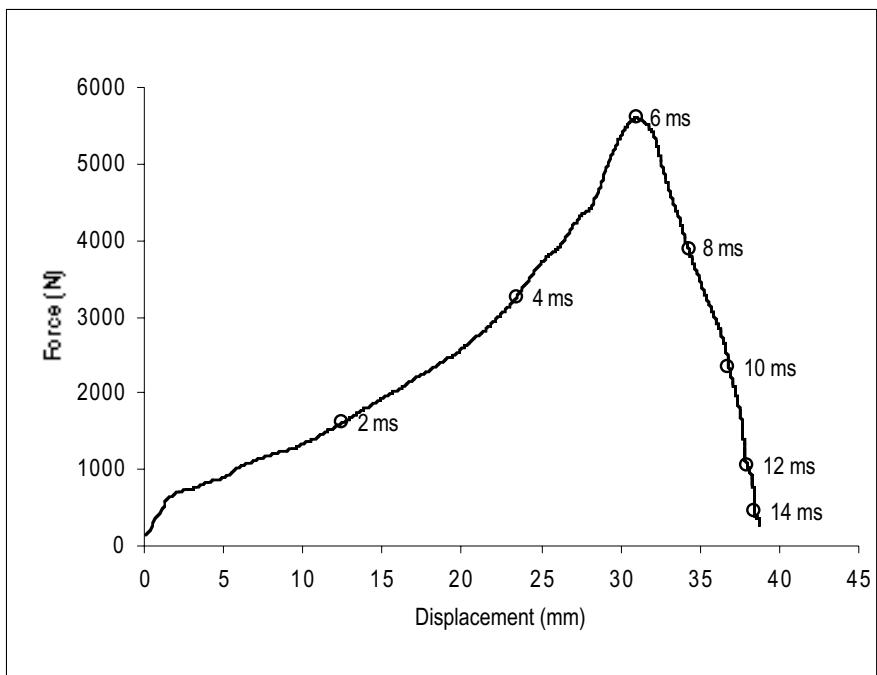


Figure A-8 The force - deflection curve for test 23050202 (50 g/l headband, Beam 2).

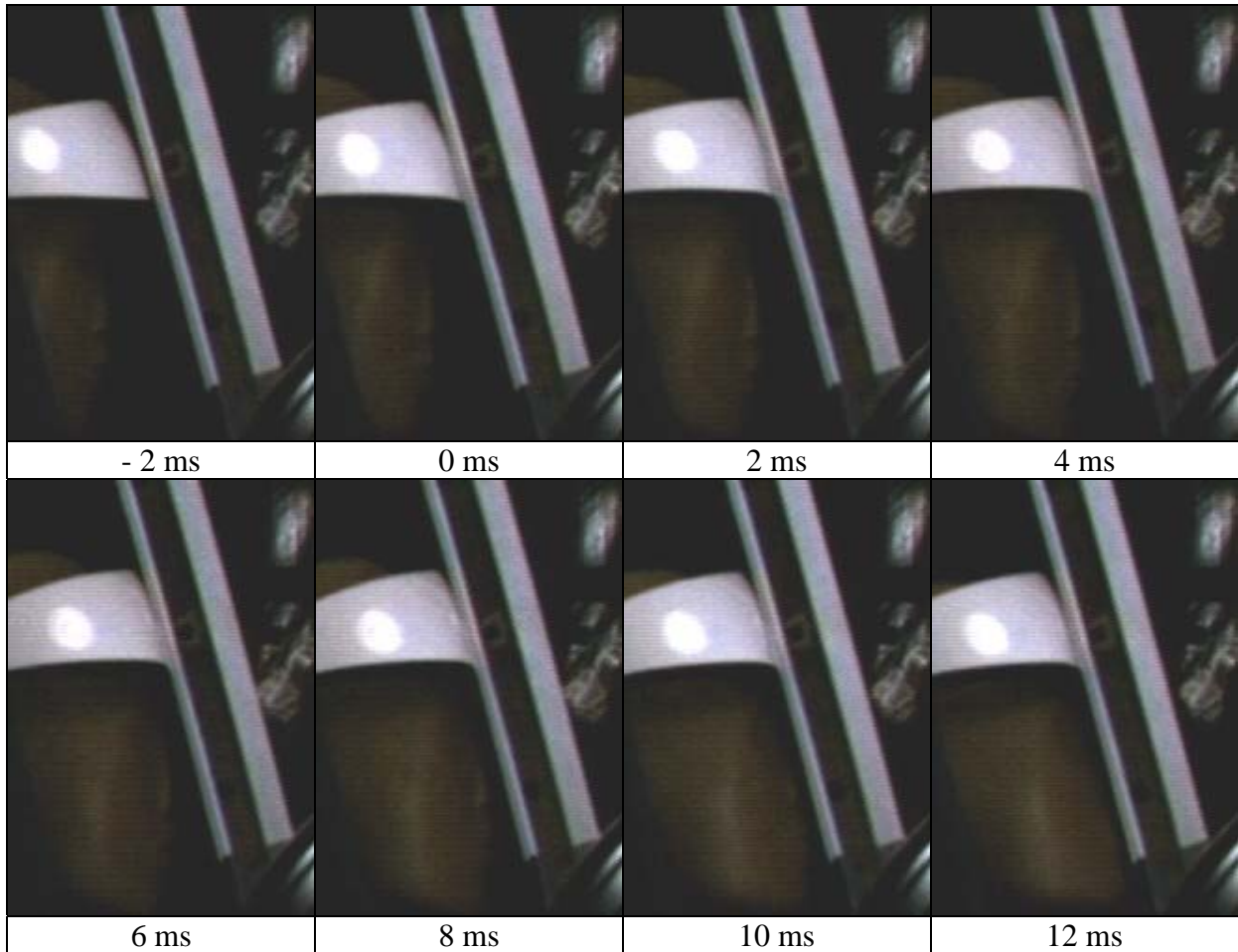


Figure A-9 High speed video images for test 23050205 (70 g/l headband, Beam 3).

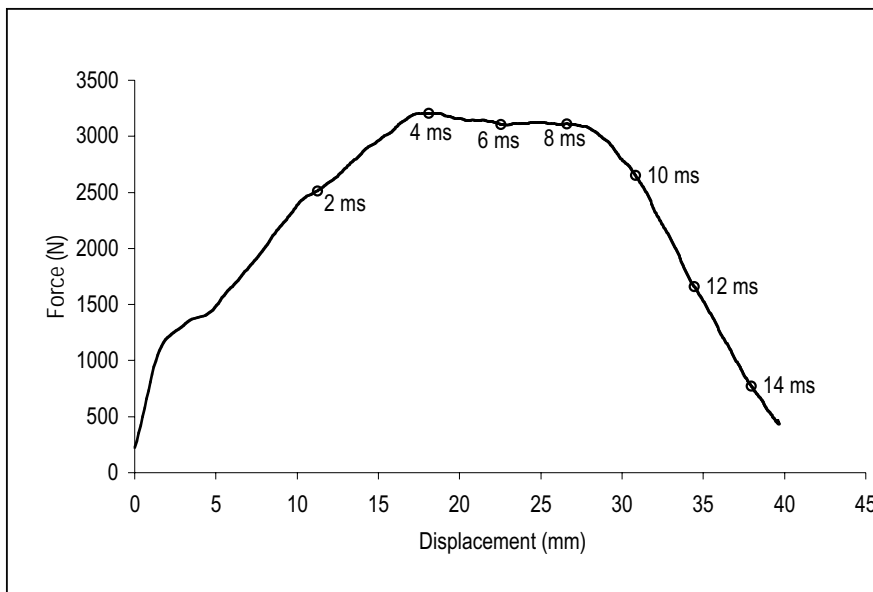
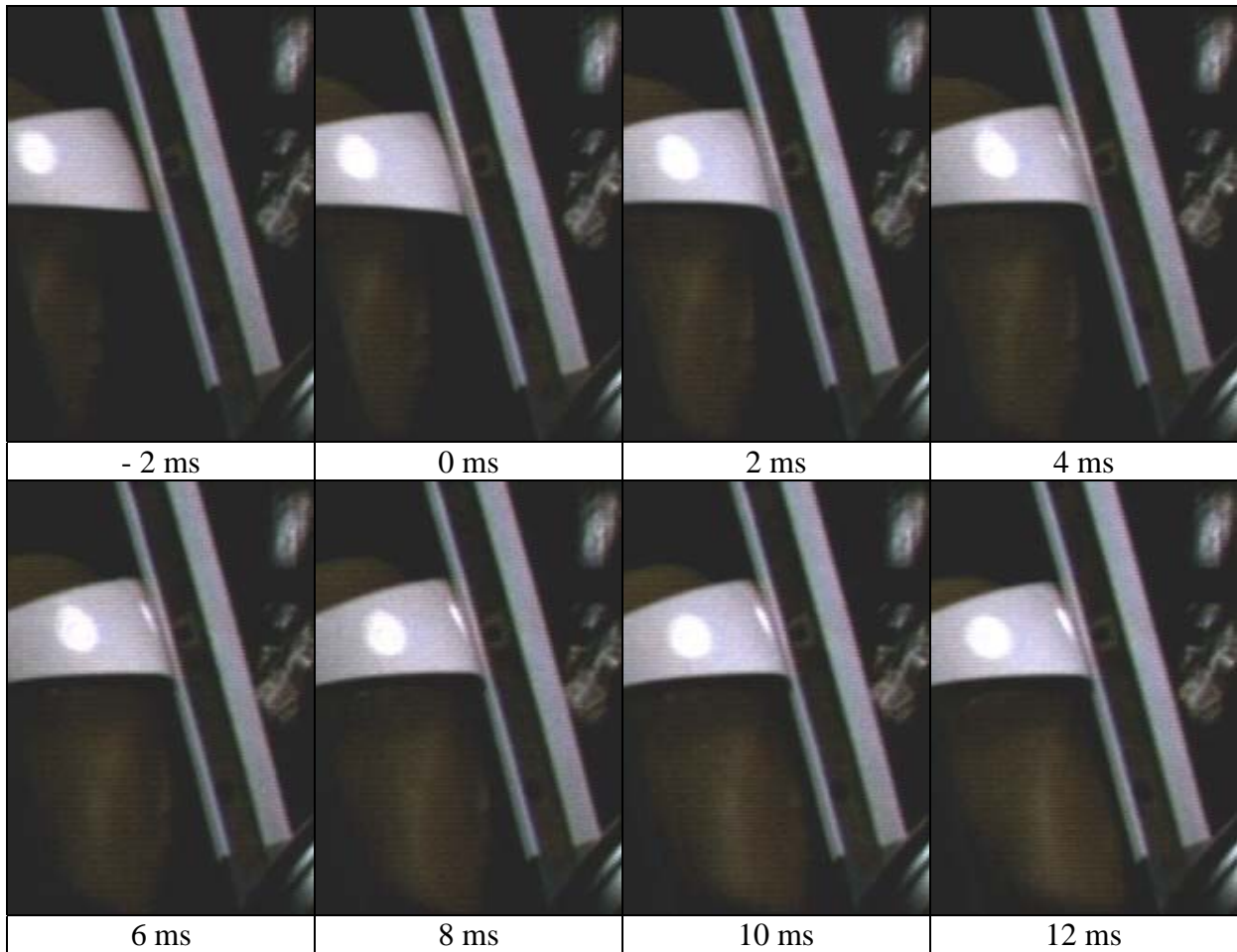


Figure A-10 The force - deflection curve for test 23050205 (70 g/l headband, Beam 3).



A-11 High speed video images for test 23050206 (50 g/l headband, Beam 3).

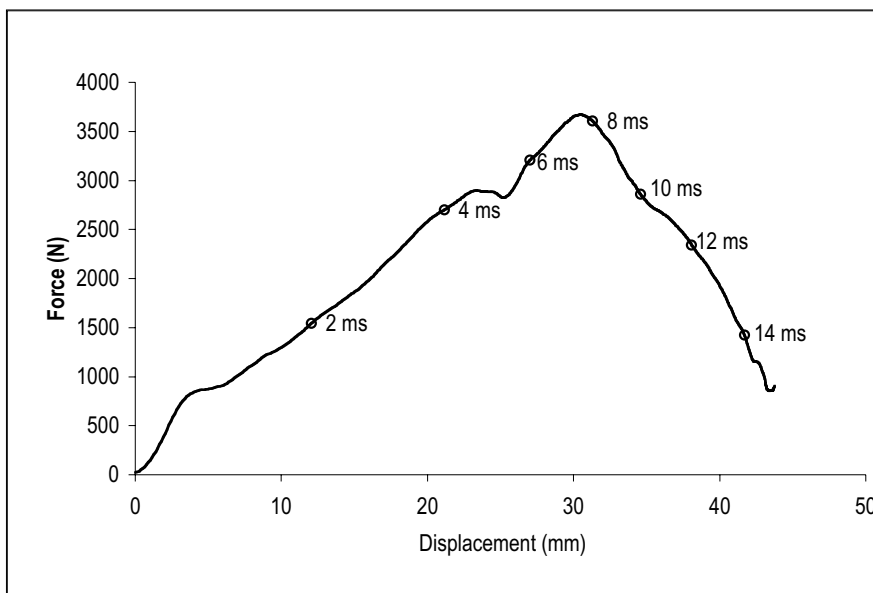


Figure A-12 The force - displacement curve for test 23050206 (50 g/l headband, Beam 3).